Biomedicine & Pharmacotherapy 83 (2016) 290–301

Available online at
ScienceDirect
www.sciencedirect.com

Elsevier Masson France
EM|consulte
www.em-consulte.com/en

The combination of bleomycin with suicide or *interferon-β* gene transfer is able to efficiently eliminate human melanoma tumor initiating cells

Chiara Fondello[a], Lucrecia Agnetti[a], Marcela S. Villaverde[a], Marina Simian[b], Gerardo C. Glikin[a], Liliana M.E. Finocchiaro[a,*]

[a] *Unidad de Transferencia Genética, Instituto de Oncología "Ángel H. Roffo", Universidad de Buenos Aires, Argentina*
[b] *Instituto de Nanosistemas and CEDESI, Universidad Nacional de San Martín, Argentina*

ARTICLE INFO

Article history:
Received 1 April 2016
Received in revised form 23 May 2016
Accepted 16 June 2016

Keywords:
Spheroids
Melanoma
HSV-thymidine kinase
Interferon-β
Bleomycin

ABSTRACT

We explored the potential of a chemogene therapy combination to eradicate melanoma tumor initiating cells, key producers of recurrence and metastatic spread. Three new human melanoma cell lines, two obtained from lymph nodes and one from spleen metastasis were established and characterized. They were cultured as monolayers and spheroids and, in both spatial configurations they displayed sensitivity to single treatments with bleomycin (BLM) or human *interferon-β (hIFNβ)* gene or herpes simplex virus thymidine kinase/ganciclovir suicide gene (SG) lipofection. However, the combination of bleomycin with *SG* or *hIFNβ* gene transfer displayed greater antitumor efficacy. The three cell lines exhibited a proliferative behavior consistent with melan A and gp100 melanoma antigens expression, and BRAF V600E mutation. BLM and both genetic treatments increased the fraction of more differentiated and treatment-sensitive cells. Simultaneously, they significantly decreased the sub-population of tumor initiating cells. There was a significant correlation between the cytotoxicity of treatments with BLM and gene transfer and the fraction of cells exhibiting (i) high proliferation index, and (ii) high intracellular levels of reactive oxygen species. Conversely, the fraction of cells surviving to our treatments closely paralleled their (i) colony and (ii) melanosphere forming capacity. A very significant finding was that the combination of BLM with *SG* or *hIFNβ* gene almost abrogated the clonogenic capacity of the surviving cells. Altogether, the results presented here suggest that the combined chemo-gene treatments are able to eradicate tumor initiating cells, encouraging further studies aimed to apply this strategy in the clinic.

1. Introduction

Malignant melanoma is an extremely aggressive form of skin cancer whose incidence continues to increase worldwide [1]. While surgical excision can cure localized disease, once distant metastasis has occurred, the overall median survival is about 6–9 months [2]. Melanoma is also among the most common causes of "metastatic cancer of unknown primary", which may reflect a rapid growth of poorly differentiated lesions arising from indolent or unrecognized cutaneous primary lesions [3].

Melanoma control is frequently short lived even when some drugs are proven to be effective. For example, the BRAF inhibitor vemurafenib is approved for the treatment of patients whose melanoma harbors the V600E mutation, which is thought to be a driver mutation [4,5]. However, after treatment with vemurafenib, cancer progression occurs within six months in the vast majority of these patients. On the other hand, the development of ipilimumab immunotherapy displayed an improvement in patients survival [6] while new strategies as oncolytic viruses produced a longer response rates in patients with advanced melanoma [7].

Despite the advances in melanoma research and drug development, 10–20% of clinically disease-free patients relapse 5–10 years following an initial treatment [8]. This phenomenon, which is known as tumor dormancy [8,9], has been related to the existence of therapy-resistant cells with stem-like activity [10,11]. The cancer stem cell theory suggests that rare tumorigenic cells, resistant to conventional therapy, are responsible for relapse, tumor progression and increased tumor aggressiveness. However, in melanoma, tumorigenic capacity is not restricted to a small

* Corresponding author at: Unidad de Transferencia Genética, Instituto de Oncología "A. H. Roffo"—UBA, Av. San Martín 5481, 1417 Buenos Aires, Argentina.
E-mail address: finolili@hotmail.com (L.M.E. Finocchiaro).

http://dx.doi.org/10.1016/j.biopha.2016.06.038
0753-3322/

subpopulation of melanoma cells but is widely shared among phenotypically diverse cells [12,13]. Furthermore, the increased plasticity and heterogeneity, is a marker of melanoma malignancy contributing to therapy failure and disease progression [13–15]. Taking into account that the therapeutic choices for melanoma are limited and most treatments fail to improve the quality of life or survival time in a meaningful way [4,5], the discovery and identification of novel therapeutics is urgently needed.

Intratumor non-viral suicide gene therapy with thymidine kinase from the herpes simplex virus (HSV*tk*), in combination with the pro-drug ganciclovir (GCV), was early proposed for treating this malignant disease [16]. The successful eradication of tumors depends on the bystander effect, by which unmodified adjacent tumor cells are also destroyed by HSV*tk*/GCV cytotoxic effect, allowing an effective tumor regression produced by only a minority of genetically modified tumor cells [17].

Interferons (IFNs) are a family of naturally existing glycoproteins known for their antiviral, antiproliferative and immunomodulatory activities. Interferon-β (IFNβ) has antitumor effects against melanoma, and generally is more potent than IFNα [18,19]. Despite the demonstrated clinical effectiveness, the treatment with recombinant hIFNα/β protein is associated with substantial systemic toxicity that worsens the patient's quality of life and often interferes with the therapy completion (about 25% of the treated patients) [20]. The limited performance of hIFNs in cancer therapy trials may have been caused by the lack or insufficiency of sustained delivery of the protein to the tumor site. In previous studies, we demonstrated that the exogenously added recombinant human IFNβ protein (rhIFNβ) can be successfully replaced by the transfer of the corresponding gene *in vitro* [18,19]. Local non-viral delivery of the gene encoding this cytokine provides a localized slow release transgenic system that avoids the adverse events associated to the injection of high doses of recombinant interferon protein while keeping its therapeutic potential [21].

Bleomycin (BLM) is a glycopeptide antibiotic with antineoplastic activity due to its endonuclease activity [22]. The cytotoxicity of BLM, a hydrophilic agent with low capability of diffusing through the plasmatic membrane, might be related to the efficiency of drug uptake. Different strategies have been developed to bypass the cytoplasmic membrane [23,24]. In a previous report, we demonstrated that lipoplexes can efficiently facilitate the delivery of BLM into melanoma tumor cells *via* endocytosis [25].

An increasing number of studies have recently shown that immunogene therapy is not only compatible with, but may be synergistic with certain chemotherapies [26–28]. Thus, more studies to explore the combined use of these two modalities are compelling.

Most of the cancer gene therapy studies carried out on animal models use tumor cell lines that were kept in culture for many generations, making them very different from the original tumors. Here, we established and characterized three human melanoma cell lines derived from surgically excised melanoma tumors, to evaluate potential *in vivo* responses of individual spontaneous human melanomas to gene therapy. Our results suggest that bleomycin in combination with suicide or interferon gene treatment is able to effectively eradicate tumor initiating cells.

2. Materials and methods

2.1. Establishment of cell cultures from human melanoma tumors

This research work followed the tenets of the Declaration of Helsinki and all samples were obtained after informed consent from the patients. The clinical samples were approved and in accordance with the institutional review board of the *Instituto de Oncología* "*Ángel H. Roffo*", *Universidad de Buenos Aires*, Argentina. Primary cell lines derived from surgically excised lymph nodes (hM1 and hM2) and spleen metastasis (hM4) of human melanomas were obtained by mechanical disruption of tumor fragments in serum free culture medium [29]. They were cultured as monolayers and multicellular spheroids at 37 °C in a humidified atmosphere of 95% air and 5% CO_2 with DMEM/F12 medium (Invitrogen, Carlsbad, CA) containing 10% FBS (Invitrogen), 10 mM HEPES (pH 7.4) and antibiotics [29]. Serial passages were done by trypsinization (0.25% trypsin and 0.02% EDTA in PBS) of subconfluent monolayers [29].

For doubling time estimation using GraphPad Prism 6 software (GraphPad Software Inc., USA), cells were trypsinized and 5×10^4 cells were plated in duplicate in 6-well plates and cultured in normal conditions. After trypan blue staining, cells were daily counted in a Neubauer chamber.

2.2. Immunocytochemistry and BRAF mutation detection

Cells attached onto a glass slide were cultured for 48 h in the above described conditions. Cells were then washed, fixed with ethanol, re-hydrated and incubated separately with the following specific monoclonal antibodies as described by the manufacturers: antihuman melan A (BioGenex, San Ramon, CA; clone A103), antihuman S-100 (BioGenex; clone 15E2E2), antihuman GP100 (BioGenex; clone HMB45); antihuman cytokeratin (Dako; clones AE1/AE3). After washing, cells were incubated with Multi-Link immunoglobulins (BioGenex) followed by streptavidin/peroxidase conjugate and developed with 3,3′-diaminobenzidine.

DNA was extracted using the High Pure FFPET DNA Isolation Kit (Roche, Indianapolis, IN). BRAF mutational status was tested using a commercial allele-specific real-time polymerase chain reaction-based assay that can detect five point mutations in codon 600 (V600E, V600K, V600R, V600D, and V600M) when present in as little as 1% of the tissue (B-Raf Mutation Analysis Kit II for detection of B-Raf V600E/K/D/R/M Mutations—Entrogen, Woodland Hills, CA).

2.3. Plasmids and transfection efficiency

Plasmids psCMVβ*gal* (6.8 Kb) [29], psCMV*tk* (4.5 Kb) [29] and psCMV*hIFNβ* (3.9 Kb) [18] carry respectively *Escherichia coli β-galactosidase* gene (3.5 Kb), herpes simplex *thymidine kinase* (1.2 Kb) and human *IFNβ* (0.6 Kb) in the polylinker site of psCMV (3.3 Kb), downstream of the CMV promoter and upstream of poly A sequences. The plasmids (bearing the kanamycin resistance gene for selection *in Escherichia coli*) were amplified, chromatographically purified and quality assessed as described [19]. Plasmid DNA for injection was resuspended to a final concentration of 2.0 mg/ml in sterile PBS.

DC-Chol (3β[*N*-(*N*′,*N*'-dimethylaminoethane)-carbamoyl cholesterol) and DMRIE (1,2-dimyristyl oxypropyl-3-dimethyl-hydroxyethylammonium bromide) were kindly provided by BioSidus (Buenos Aires, Argentina). DOPE (1,2-dioleoyl-sn-glycero-3-phosphatidyl ethanolamine) was purchased from Sigma (Saint Louis, MO). Liposomes were prepared at lipid/co-lipid molar ratios of 3:2 (DCChol: DOPE) or 1:1 (DMRIE:DOPE) by sonication as described [18,29]. Lipids in chloroform solution were evaporated to dryness, and liposomes were prepared by reconstitution in sterile sodium phosphate buffer 0.1 M (pH 7.3) to a final concentration of 1.0 mg/ml, followed by 10 cycles of 15 s sonication at 4 °C. Before lipofection, liposomes and plasmid DNA (1:2, v:v) were mixed and allowed to complex at room temperature for 10 min. Optimal lipid mixtures were determined for every cell line.

In most experiments, cells were seeded into 12-well plates at a density of $3–5 \times 10^4$ cells/cm^2 and were allowed to adhere

overnight. Monolayers were exposed to lipoplexes (0.5 μg plasmid DNA/cm^2 and 1 μl liposome/cm^2) from 3 to 5 h in a serum-free medium. Then the lipofection medium was replaced with fresh complete medium.

To ensure that they were comparable in different experiments, transfection efficiencies were checked 24 h after lipofection by β-*galactosidase* staining with 5-bromo-4-chloro-3-indolyl β-D-galactopyranoside (X-GAL, Sigma) and further counting with an inverted phase contrast microscope [19].

2.4. Sensitivity to suicide and hIFNβ gene in vitro assays

Twenty-four hours after lipofection, with suicide gene (SG, HSV*tk*/GCV), *hIFNβ*, or β*gal* alone or co-delivered with BLM (3 mg/ml), cells were seeded on regular plates as monolayer (3.5–7.0 × 10^4 cells/ml) or on top of 1.5% solidified agar to form spheroids (1.0 × 10^5 cells/ml) and incubated with medium containing 5 μg/ml ganciclovir (Richet, Buenos Aires, Argentina). After 5 days in monolayers or 13 days in spheroids, cell viability was quantified using the acid phosphatase (APH) assay [25]. Briefly, spheroids growing in liquid overlay were transferred to 96-well microplates, washed and finally incubated for 90 min at 37 °C, with 100 μl per well of the assay buffer (0.1 M sodium acetate, 0.1% Triton-X-100, supplemented with *p*-nitrophenyl phosphate). Following incubation, 10 μl of 1 N NaOH was supplemented to each well, and absorption at 405 nm was measured within 10 min.

2.5. Flow cytometry cell cycle analysis

Three days after lipofection, with SG, *hIFNβ*, or β*gal* alone or co-delivered with BLM, cells were trypsinized, fixed in 70% (v/v) ethanol at −20 °C for 1 h, treated with RNase, stained with 10 μg/ml propidium iodide for 30 min, and subjected to single-channel flow cytometry on a Becton Dickinson FACScan (Franklin Lakes, NJ), with collection and analysis of data performed using Becton Dickinson CELLQuest software [29].

2.6. Measurement of cellular reactive oxygen species (ROS) production

Three days after lipofection with SG, *hIFNβ*, or β*gal* alone or co-delivered with BLM, cells were detached, washed with PBS and incubated with 5 μM H_2DCF-DA (Invitrogen), a cell-permeable non-fluorescent dye that in the presence of intracellular oxidants is converted to fluorescent DCF [18]. After 20 min, normal culture conditions were re-established and the cellular fluorescence intensity was analyzed by flow cytometry as described above. The final data were analyzed using the Flowing software and the medium intensity of fluorescence was calculated (Geometric Mean: Gm). The results were expressed as the Gm percentage to the untreated control cells.

2.7. Colony formation assay

Surviving cells after 6 (monolayers) or 13 days (spheroids) of chemo-gene treatments were trypsinised into single cells. Monodispersed cells were seeded at low density (400–600 cells/ml, 1000–1500 cells/well in a 6-well plate) and incubated at 37 °C with complete medium until colonies were visible. Medium was changed once a week. After 7–10 days of culture, plates were washed, fixed with 5% acetic acid in ethanol, and stained with crystal violet. The number of colonies was counted under an inverted microscope. The clonogenic capacity was defined as the percentage of cells able to grow as colonies of more than 10 cells.

2.8. Melanosphere formation assay

Surviving cells after 6 (monolayers) or 13 days (spheroids) of chemo-gene treatments were trypsinised into single cells and plated onto 12-well low attachment suspension culture plates (Greiner Bio-One, Köln, Germany) at a density of 2000–2500 viable cells/ml. Cells were grown in 1 ml serum-free media, supplemented with B27 (Gemini Bioproducts, West Sacramento, CA), and 20 ng/ml EGF [30]. Melanospheres were counted after 6–8 days in culture with a Nikon eclipse TE2000-S inverted microscope. The melanosphere forming capacity was defined as the percentage of cells able of clonal proliferation as melanospheres with more than 8 cells.

2.9. Statistics

Results were expressed as mean ± standard error of the mean (s.e.m.) (n: number of experiments corresponding to independent assays). Differences between groups were analyzed using unpaired Student's *t*-test (if two groups), One-way ANOVA followed by Tukey's test (if more than two groups) or two-way ANOVA followed by Bonferroni test (if two nominal variables). Correlations were determined by Pearson test with GraphPad Prism program (GraphPad Software Inc., USA). $p < 0.05$ values were considered statistically significant.

3. Results

3.1. Melanoma derived cell lines displayed considerable heterogeneity

Three human melanoma cell lines, derived from patient tumor tissue were successfully established. They derived from surgically excised lymph nodes (hM1 and hM2) or spleen (hM4) metastases and were maintained in culture for over 60 passages.

By determining duplication times (DT) in standard culture medium, we found a fast (hM1), an intermediate (hM4) and a slow (hM2) growing melanoma cell line (Table 1). This significantly

Table 1
Characteristics of cultured melanoma cells.

Cell line	Duplication time (h)/[n]	PI (%)/[n]	ROS (geometric mean)/[n]	Clonogenic capacity (%)/[n]	Melanospheres forming capacity (%)/[n]	Lipofection rate (%)/[n]
hM1	24.4 ± 0.6/[3]	18.8 ± 1.5/[12]	33.2 ± 4.5/[20]	2.3 ± 0.2/[32]	9.0 ± 0.6/[12]	8.0 ± 1.2/[33]
hM2	33.3 ± 0.4/[3]	14.2 ± 1.6/[11]	73.6 ± 7.0/[18]	14.6 ± 1.6/[46]	–	3.4 ± 0.6/[24]
hM4	28.3 ± 0.1/[3]	31.4 ± 1.5/[7]	153.3 ± 20.7/[10]	1.2 ± 0.1/[6]	3.8 ± 0.4/[8]	0.4 ± 0.1/[7]
hM1 vs. hM2	$p < 0.0001$	$p < 0.05$	$p < 0.0001$	$p < 0.0001$	–	$p < 0.005$
hM1 vs. hM4	$p < 0.0004$	$p < 0.0001$	$p < 0.0001$	$p < 0.05$	$p < 0.0001$	$p < 0.01$
hM2 vs. hM4	$p < 0.0001$	$p < 0.0001$	$p < 0.0001$	$p < 0.005$	–	$p < 0.01$

Time course of growth was determined by trypan blue exclusion cell counting and lipofection efficiency was measured as blue X-Gal stained cells as described in Materials and methods. Proliferation index (PI) of untreated cells was determined by evaluating the percentage of cells in the S, G2/M and hyperdiploid phases. ROS: Reactive oxygen species.

Table 2
Tumor markers and morphology of cultured human melanoma cells.

Cell line	CD68	S100	Melan A	gp100	Cytokeratin	BRAF	Cell type	Origin
hM1	–	+++	+++	+	–	V600E	FS	LN mts
hM2	–	+++	++	+	+	V600E	EP	LN mts
hM4	–	+++	++	+	–	wt	FS	spleen mts

Cells growing for 3 days in monolayer were fixed and treated for markers staining or BRAF mutation (V600E) as described in Materials and methods. wt: wild type; LN: lymph node; mts: metastasis; FS: fibroblastic; EP: epithelioid. The number of + symbols represent a semi-quantitative estimation of the relative staining of each individual tumor marker among the three cell lines.

longer DT for hM2 was consistent with the lower proliferation index (PI) as the number of cells in S, G2/M and hyperdiploid phases. In addition, hM2, that formed 5- and 10-fold more colonies than hM1 and hM4, was not able to form melanospheres (MS) when plated in serum-free media in low attachment suspension culture plates. Accordingly, hM2 cells exhibited a more epithelial morphology and a tight cell-to-cell and cell-substrate interactions (Table 2). Conversely, hM1 and hM4 showed fibroblastic shaped cells and scattered monolayers (mnl) that were easily detached by Ca^{2+} depletion (Table 2). Moreover, hM4 cells, with the highest basal proliferation index (PI) and intracellular reactive oxygen species (ROS), exhibited the lowest clonogenic and melanosphere forming capacity.

All these basal parameters of untreated cell lines are in agreement with the high heterogeneity commonly seen in melanomas [13–15].

3.2. Cultured cell lines expressed melanoma specific markers

Melanocytes arise from embryonic neuroectoderm and retain the ability to differentiate into spindled or epithelioid cells, being identification of melanoma difficult in poorly differentiated amelanotic tumors. Specific markers can help in the diagnosis. As shown in Fig. 1, S100, an isoform of a calcium binding protein restricted to neuroectodermal cells, was high in the three cell lines. Melan A (expressed in pigmented cells) and gp100 (expressed in activated melanocytes) are two specific and sensitive melanoma antigens associated with cell proliferation programs [31,32]. Melan A was high in hM1 and moderate in hM2 and hM4. Besides, the three lines also co-expressed gp100, suggesting a proliferative behavior. Cytokeratin (a keratinocyte specific marker) was low in hM1 and hM4, but high in the epithelial-like hM2. On the other hand, the three cell lines were negative for CD68 (lysosome-associated glycoprotein). Taking into account the therapeutic relevance of BRAF, we evaluated its mutation status. While hM4 had the wild type genotype, hM1 and hM2 presented the BRAF V600E mutation (Table 2).

Thus, morphologic analysis and the positive staining for most of the assayed markers (Table 2) confirmed the previous histopathological diagnosis of melanoma.

3.3. Melanoma cells grew in vitro as multicellular spheroids

Multicellular tumor spheroids are heterogeneous cellular aggregates that are considered valid models to recapitulate features of tumor microregions or micrometastases [29]. The three cell lines were able to grow as multicellular spheroids (Fig. 2). While in hM2 and hM4 spheroids cells appeared intimately

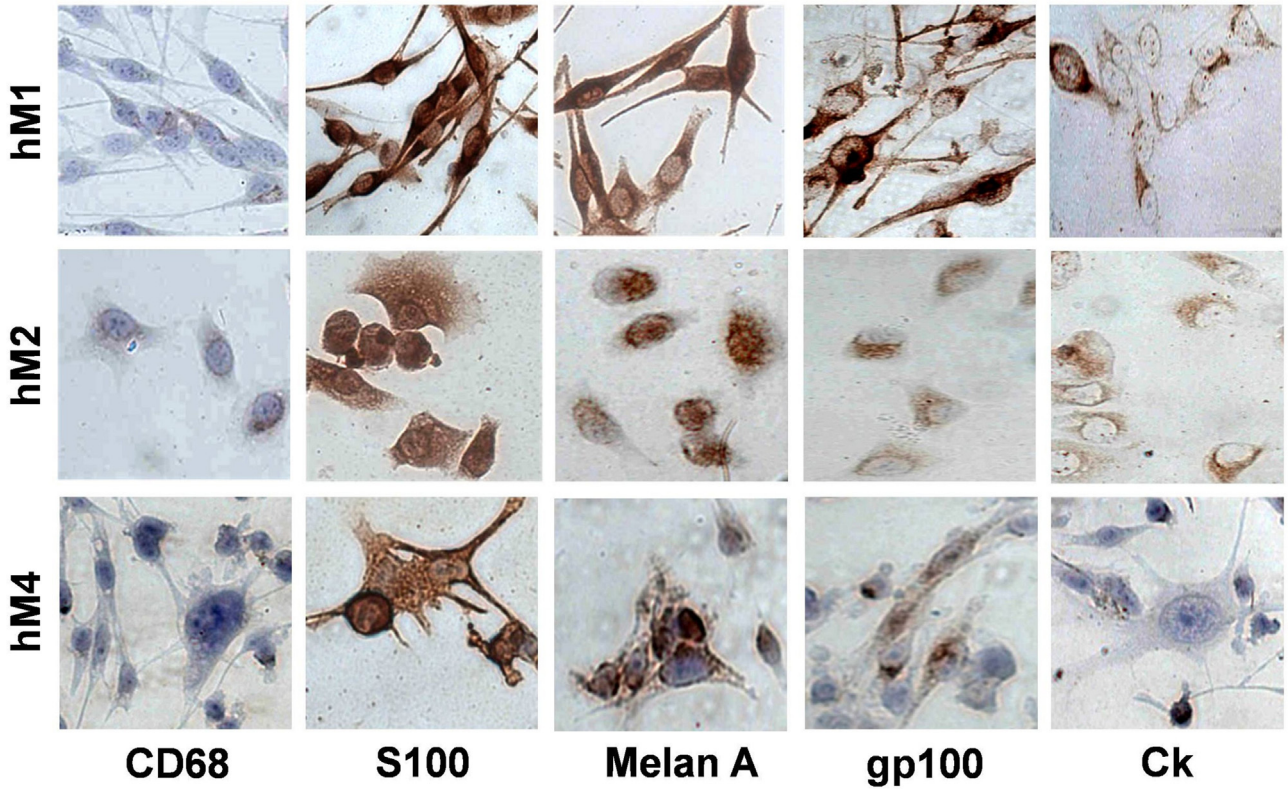

Fig. 1. Detection of melanoma specific antigenic markers by immunocitochemistry. Cells growing for 2 days onto glass slides were fixed and stained with specific antibodies against CD68, S100, Melan A, gp100 and cytokeratin (Ck), as described in Materials and methods, and photographed (200×).

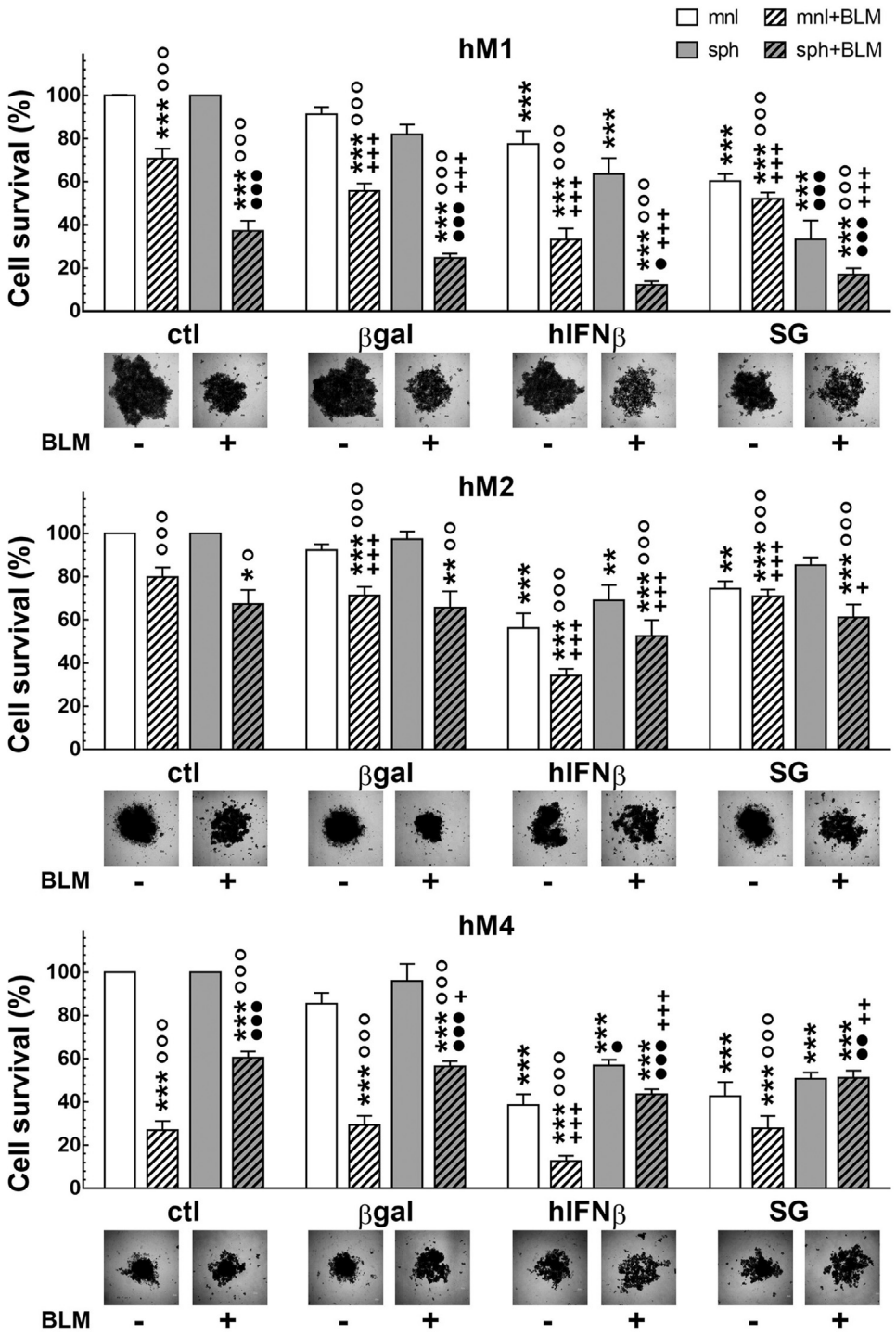

Fig. 2. Cytotoxic effects of bleomycin (BLM), human *interferonβ*- (h*IFNβ*) gene and suicide gene (SG) system (HSV*tk*/GCV) on monolayers and spheroids of human melanoma cells. The assay was performed as described in Materials and methods. The results represent means ± s.e.m. of n = 20 (hM1 and hM2), and n = 6 (hM4) independent experiments. In this case each value was relative to the respective control (ctl) condition: monolayers (mnl) or spheroids (sph). * *vs* the respective *β-galactosidase* gene (β*gal*); ° BLM *vs* their respective value without BLM; + BLM/genes combined treatments *vs* their respective ctl + BLM; ● sph *vs* their respective value in mnl. One symbol: $p < 0.05$, two symbols: $p < 0.01$, three symbols: $p < 0.001$.

Lower panels: Images represent individual human melanoma spheroids treated as described in the bar plots. Spheroids growing in suspension in 96-well plates for 13 days were photographed using an inverted phase contrast microscope (40×).

associated with each other and closely packed, in hM1 they appeared as loosely associated aggregates where single cells could be clearly distinguished (Fig. 1).

3.4. Melanoma cells displayed considerable response diversity to the assayed treatments

Simultaneous attack of different therapeutic targets often constitutes an effective strategy for the treatment of the oncologic patient. Thus, we explored if both, human *interferon-β* (*hIFNβ*) gene and herpes simplex *thymidine kinase*/ganciclovir (HSV*tk*/GCV) suicide gene (SG) therapy could be successfully combined with bleomycin (BLM) for treating the human melanoma derived cell lines.

We estimated the SG cytotoxicity at the pharmacologically relevant 5 μg/ml ganciclovir (GCV) concentration, similar to an intratumor standard dose for our canine patients [33]. As shown in Fig. 2, the tested cell lines were sensitive to both, *hIFNβ* and SG lipofection in both spatial configurations (hM2 sph excluded).

Lipofection rates were <10% in the three cell lines (Table 1). Even though variability in lipofection efficiencies of cell lines could explain the heterogeneity of the responses, no correlation was observed between gene cytotoxicity and their lipofection efficiencies. The hM1 cell line, with lipofection efficiency of about 8%, was more sensitive to SG system in both spatial configurations. On the other hand, hM2 presenting very low lipofection efficiency (about 3%), was less (mnl) or no sensitive (sph) to SG system and more sensitive to *hIFNβ* gene in both spatial configurations. The remaining cell line, hM4, exhibited similar susceptibility to both *hIFNβ* and SG in both spatial configurations. Surprisingly, this line with fair lipofection efficiency (<1%), displayed the highest sensitivity to both *hIFNβ* and SG gene when growing as monolayers.

Interestingly, the three lines were sensitive to BLM alone in both spatial configurations. However, control lipofection (β*gal*) enhanced BLM cytotoxicity in the three lines: hM1 (both spatial configurations), hM2 (mnl) and hM4 (sph). This effect was probably due to lipoplexes mediated cellular uptake [25]. On the other hand, the combination with BLM enhanced the individual effects of both, *hIFNβ* and SG gene, in the three lines in both spatial configurations (hM4 sph excluded). Even the SG insensitive hM2 spheroids displayed increased sensitivity to the BLM/SG combination. Lastly, the highest antitumor effects were found with the combination of hIFNβ plus BLM, in the three lines in both spatial configurations.

With the exception of hM1, hM2 and hM4 showed equal or greater response to our chemo-gene treatments as monolayers than as their respective spheroids. This decreased sensitivity of spheroids would be based on the phenomenon called multicellular resistance (MCR) that reflects the relative intrinsic treatment-resistant phenotype of most solid tumors growing *in vivo* [29].

Microscopic monitoring of treated spheroids (Fig. 2) paralleled the results obtained by the APH assay (see Materials and methods).

3.5. The treatments increased the fraction of cycling cells

In a previous paper we demonstrated that, in opposition to the treatment, there is a repopulation (re-growth) mechanism whose strength would be intrinsic of each individual tumor [29].

Here, we observed that, in these three human melanoma lines, our chemo-gene treatments enhanced the proliferative phenotype of these cells which subsequently led to increased sensitivity to these therapeutic agents (Fig. 3a). This was confirmed by the correlation between the fraction of cells exhibiting high proliferation index (PI) and the extent of the cytotoxic response of our treatments (Fig. 3b,c,d).

The hM2 cell line, that manifested the highest re-growth resistance phenotype, exhibited a high inverse correlation ($p < 0.0003$) between PI and hM2 cell survival to all the treatments in both spatial configurations (mnl: $R^2 = 0.878$, sph: $R^2 = 0.917$). The correlation was maintained when the treatments were analyzed separately: the genetic treatments (mnl: $R^2 = 0.982$, sph: $R^2 = 0.935$; $p < 0.02$) and BLM/genes combined treatments (mnl: $R^2 = 0.936$, sph: 0.935; $p < 0.02$).

On the other hand, hM1 showed an inverse correlation between PI and cell survival to both, genetic treatment (mnl: $R^2 = 0.982$, sph: $R^2 = 0.981$; $p < 0.02$) and BLM/genes combined treatments (mnl: $R^2 = 0.896$, sph: $R^2 = 0.974$; $p < 0.03$). However, no correlation was found when all the treatments were compared collectively.

Even hM4, with the highest basal levels of cycling diploid and hyperdiploid cells, increased the proportion of cells with high PI in response to the treatments. This cell line also displayed a significant correlation between PI and cell survival to all the treatments in both spatial configurations (mnl: $R^2 = 0.75$, sph: $R^2 = 0.76$; $p < 0.004$). The PI also correlated with hM4 survival to genetic treatments in spheroids ($R^2 = 0.8699$; $p = 0.037$), but no correlation was found in monolayers. A direct correlation between PI and hM4 spheroid survival to genes/BLM combined treatments would be likely ($R^2 = 0.7712$, $p = 0.06$). These data, and those of hM1 (all treatments), suggest that the higher cytotoxicity of the combined chemo-gene treatments could be due to its ability (i) to kill both dividing and quiescent cells or (ii) to promote proliferation of melanoma cells, and therefore increasing their sensitivity to these therapeutic agents.

3.6. The treatments increased the fraction of cells with high ROS levels

Reactive oxygen species play a major role in cellular proliferation, differentiation and survival [34,35]. High ROS state is linked with proliferative activity and cell differentiation [34–37].

Previous results from our laboratory [18,19] indicate that *IFNβ*-lipofection increases ROS concentration in human and canine melanoma cell lines. Thus, we explored a possible link between an increase in ROS and treatment cytotoxicity in our new established cell lines.

As seen in Fig. 4a, the treatments that significantly decreased cell viability increased the subpopulation of cells with high intracellular ROS levels in the three cell lines. As with PI, the rise in ROS levels correlated with the extent of the cytotoxic response. The three cell lines exhibited an inverse correlation ($p < 0.05$) between intracellular ROS levels and cell survival to the chemo-gene treatments in both spatial configurations (Fig. 4b).

3.7. Surviving tumor cells displayed a reduced clonogenic capacity after treatments

After seeding the same number of surviving cells, we found that hM2 formed respectively 5- and 10-fold more colonies than hM1 and hM4, suggesting that hM2 could have a higher proportion of tumor initiating cells (TIC) (Table 1 and Fig. 5).

As shown in Fig. 5, all the treatments that significantly decreased cell viability, decreased the clonogenic capacity of the surviving cells after treatments. It is worth to note that the clonogenic capacity of surviving cells of the three cell lines almost disappeared (hM1 and hM2) or disappeared after treatment with BLM alone or combined with genes (Fig. 5a).

The morphology of the clones was variable. While hM2 tended to form spherical aggregates and hM4 elongated aggregates, hM1 tended to form both spherical and elongated aggregates (Fig. 5b). The hM2 cell line formed growing colonies that after 2 or 3 weeks produced bigger colonies, visible in plain sight. Conversely, hM1

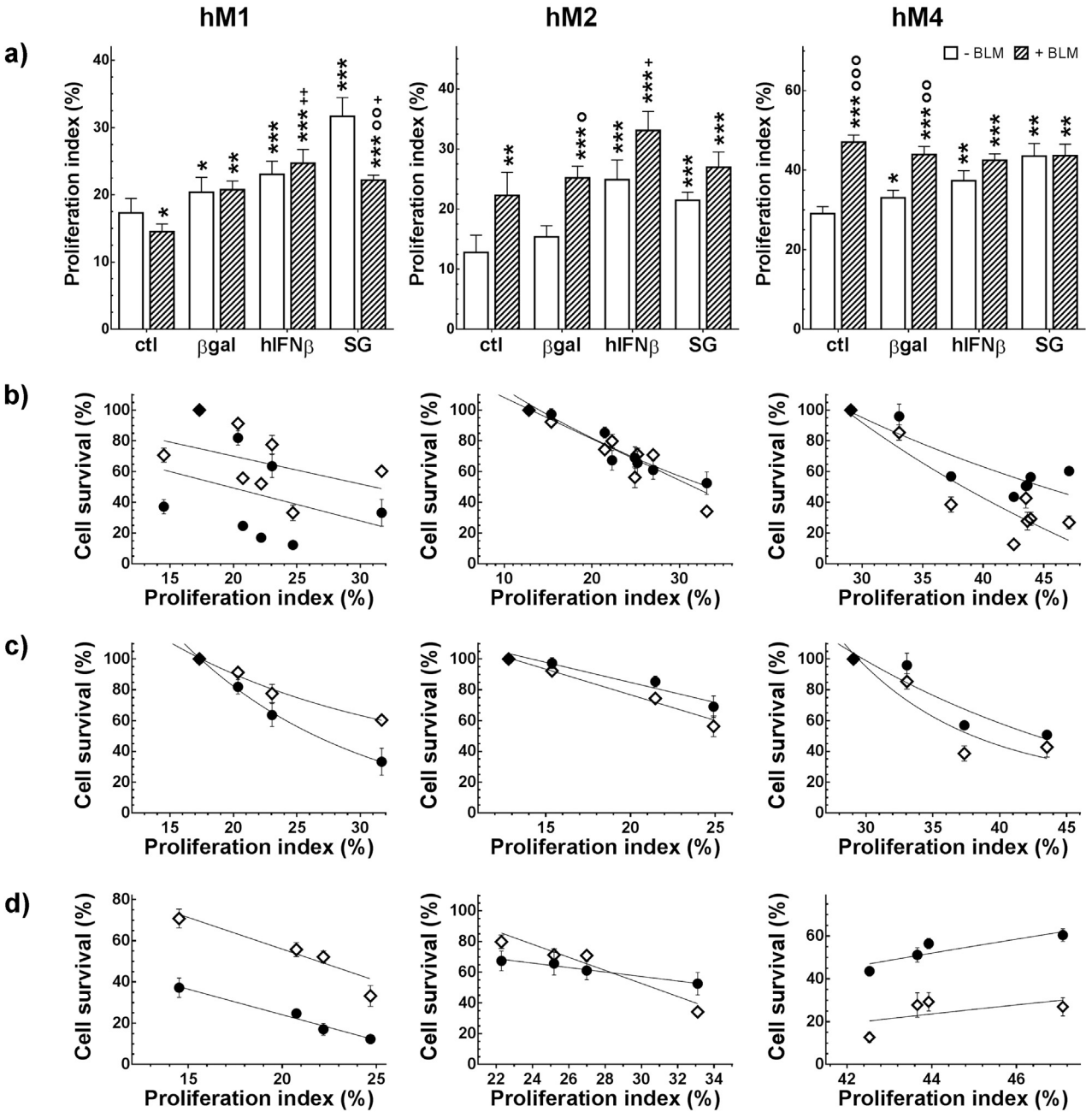

PI	hM1	mnl	sph	hM2	mnl	sph	hM4	mnl	sph
b)	R^2	0.205 (lin) ns	0.130 (lin) ns	R^2	0.878 (lin) ***	0.928 (exp) ****	R^2	0.75 (log) **	0.76 (log) **
c)	R^2	0.982 (log) **	0.99 (exp) **	R^2	0.982 (lin) **	0.935 (lin) *	R^2	0.633 (log) ns	0.87 (exp) *
d)	R^2	0.896 (lin) *	0.974 (lin) **	R^2	0.936 (lin) *	0.973 (lin) **	R^2	0.3 (exp) ns	0.771 (log) ns

Fig. 3. Effects of SG (HSV*tk*/GCV) and h*IFNβ* lipofection in the absence or presence of BLM on the proliferation index of melanoma cells. Cells growing for 5 days as monolayers were suspended, treated and subjected to flow cytometry analysis as described in Materials and methods. The proliferation index (PI) was determined by evaluating the percentage of cells in the S, G2/M and hyperdiploid phases. (a) The results represent means ± s.e.m. of n = 6 (hM1 and hM2), and n = 4 (hM4) independent experiments. * *vs* their respective ctl; ° BLM *vs* their respective value without BLM; + BLM/genes combined treatments *vs* their respective ctl + BLM. Correlations between PI and cells survival (from Fig. 2) in mnl (◇) or sph (●) to all the treatments (b), or to the treatments without (c) or with BLM (d) were determined by Pearson test with GraphPad Prism program. One symbol: $p < 0.05$, two symbols: $p < 0.01$, three symbols: $p < 0.001$. Correlation functions: lin, linear; log, logarithmic; exp, exponential. See other abbreviations in Fig. 2.

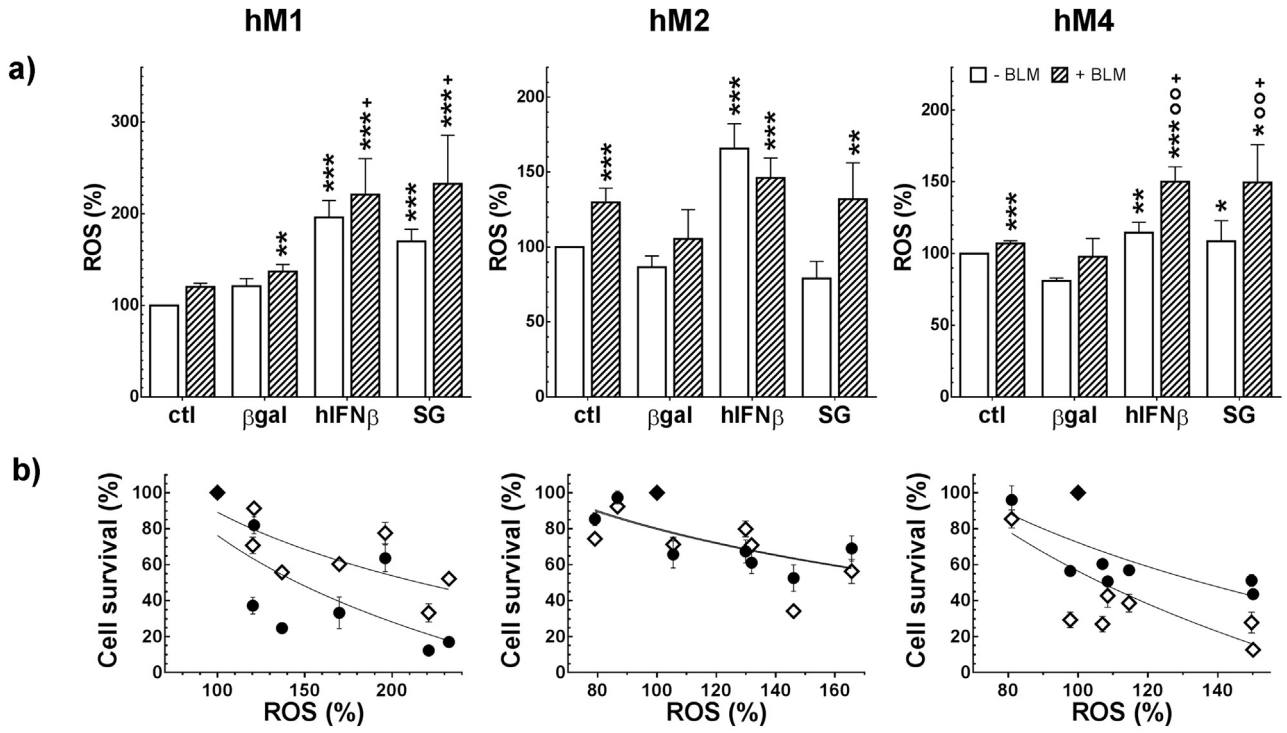

ROS	hM1	mnl	sph	hM2	mnl	sph	hM4	mnl	sph
b)	R^2	0.57 (log) *	0.5 (exp) *	R^2	0.47 (lin) *	0.54 (log) *	R^2	0.55 (exp) *	0.53 (exp) *

Fig. 4. Effects of SG (HSV*tk/GCV)* and h*IFNβ* lipofection in the absence or presence of BLM on intracellular reactive oxygen species (ROS) production by melanoma cells. Intracellular ROS levels were measured by means of H2DCF-DA probe as described in Materials and methods. (a) The results represent means ± s.e.m. of n = 6 (hM1 and hM2), and n = 3 (hM4) independent experiments. * *vs* their respective β*gal*; ° BLM *vs* their respective value without BLM; ⁺ BLM/genes combined treatments *vs* their respective β*gal* + BLM. (b) Correlations between ROS levels and cells survival (from Fig. 2) to all treatments in mnl (◇) or sph (●) were determined by Pearson test with GraphPad Prism program.
One symbol: $p<0.05$, two symbols: $p<0.01$, three symbols: $p<0.001$. See abbreviations in Fig. 2.

and hM4 colonies did not persist over time in growing medium, undergoing cell death after two weeks (Fig. 5b).

A notable finding was the direct correlation between the fraction of surviving cells after any treatment and the clonogenic efficiency in the three cell lines. There was a higher correlation ($p < 0.0004$) of clone forming capacity of surviving cells when growing as spheroids in the three cell lines (Fig. 5c).

3.8. Surviving tumor cells decreased their melanosphere forming capacity

Cancer treatments such as chemo and radiotherapy have been shown to lead to an increase of cells with stem cell properties such as self-renewing capacity [36].

However, few reports have addressed whether gene and chemo-gene treatments sensitize this particular cell population [38]. To answer this question, we carried out melanosphere assays with the treatment-resistant surviving cells. In these assays, we were able to identify melanosphere forming capacity (MFC) in hM1 and hM4 human melanoma cell lines. All cytotoxic treatments decreased the number and size of MS derived from surviving cells. In hM1, the combination with BLM enhanced the individual effect of both SG and *hIFNβ* gene. A very dramatic decrease of MS initiating subpopulation of hM1 surviving cells was found after the BLM/*hIFNβ* combined treatment (Fig. 6a).

As shown in Fig. 6a,b, hM1 cells displayed better MFC than hM4 cells. On the other hand hM2 cells, that readily formed spheroids when plated on top of solidified agar, were not able to form MS under non-adherent and serum-free conditions. While hM1 and hM4 cells displayed a MS-growing phenotype (Fig. 6**b**), hM2 cells grew as an adherent phenotype under the same culture conditions (data not shown).

When seeded in a growing medium favorable for adhesion (supplemented with 10% of FBS), hM1 MS from untreated control, βgal- and hIFNβ-expressing cells, disassembled and grew as a monolayer, reaching confluence in about 3, 3 and 6 weeks respectively. These control, βgal- and hIFNβ-expressing MS cells had the ability to form secondary MS. The same number of MS cells produced less secondary MS than their primary counterparts (data not shown). Conversely, other treatments produced smaller hM1 MS that did not last as long in the growing medium (data not shown). On the other hand, hM4 small MS when seeded onto an adherent substrate with growing medium did not disassemble. Regardless of the pretreatment, hM4 MS remained as non-growing MS for up to 3 months (n = 3, data not shown).

Cells derived from hM1 control MS were separately cultured for over 30 passages in the FBS supplemented medium. This new hM1MS line variant exhibited similar or lower self-renewing capacity than hM1 (Fig. 6a).

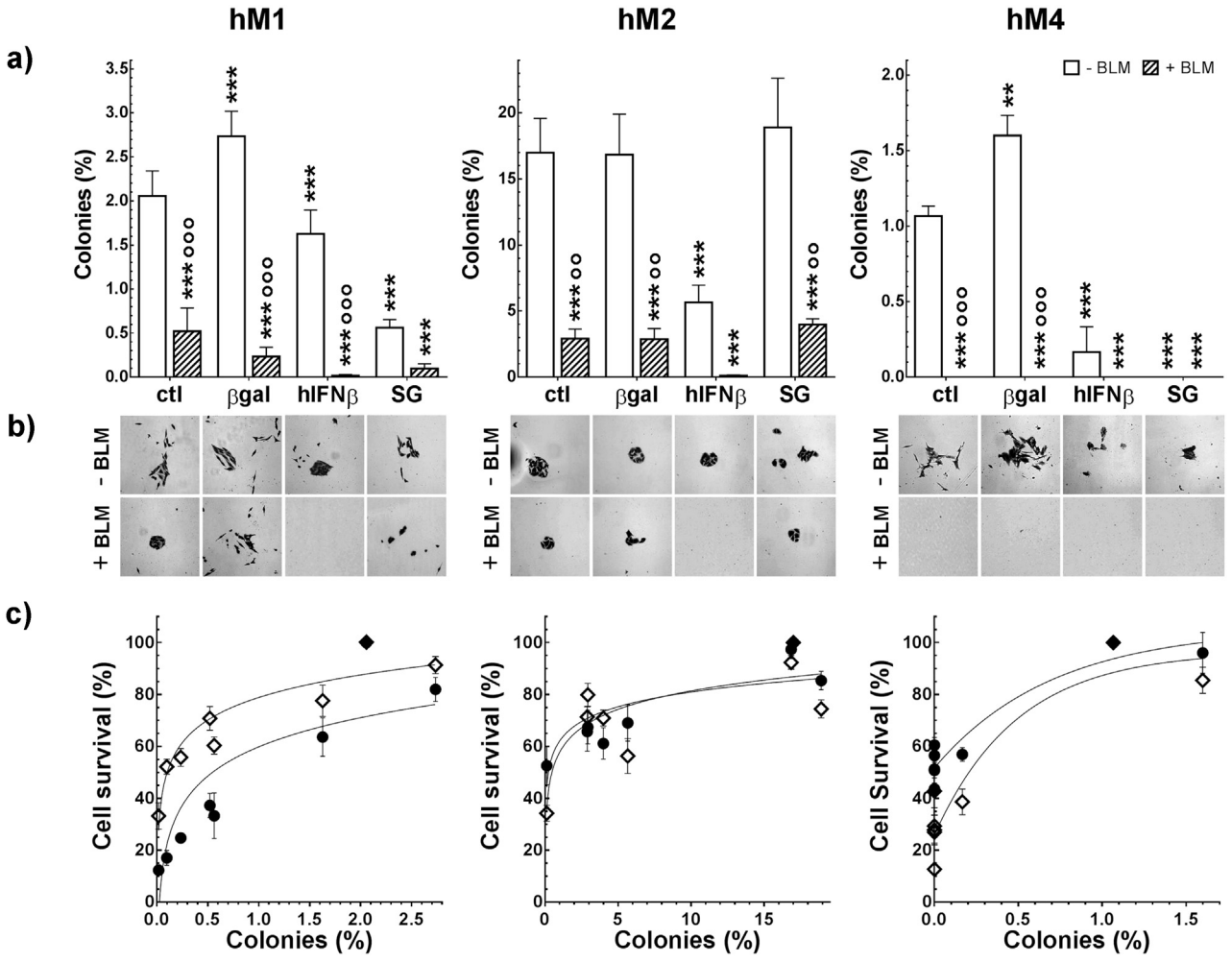

	hM1	mnl	sph	hM2	mnl	sph	hM4	mnl	sph
c)	R^2	0.88 (log) **	0.88 (lin) ***	R^2	0.69 (log) *	0.87 (lin) ***	R^2	0.81 (exp) **	0.875 (lin) ***

Fig. 5. Clonogenic capacity of the surviving melanoma cells to SG (HSV*tk*/GCV) and h*IFNβ* lipofection in the absence or presence of BLM. (a) Clonogenic capacity of hM1, hM2 and hM4 treatment surviving cells (relative to the number of seeding cells) assessed at day 6 (mnl) or 13 (sph) after seeding at low density as described in Materials and methods. The results represent means ± s.e.m. of n = 12 (hM1 and hM2), and n = 3 (hM4) independent experiments. * *vs* their respective ctl; ° BLM *vs* their respective value without BLM; + BLM/genes combined treatments *vs* their respective ctl + BLM. (b) Representative examples of colony forming activity by the three human lines treated as described in the bars plot. (c) Correlations between the clonogenic capacity and cells survival (from Fig. 2) to all treatments in mnl (◇) or sph (●) determined by Pearson test with GraphPad Prism program.
One symbol: $p < 0.05$, two symbols: $p < 0.01$, three symbols: $p < 0.001$. See abbreviations in Fig. 2.

A significant finding was the high correlation between the amount of cells surviving treatments and the number of MS in both spatial configurations for hM1, hM4 and hM1MS (Fig. 6c).

4. Discussion

Here, we established and characterized three human melanoma cell lines obtained from lymph nodes (hM1 and hM2) and spleen metastasis (hM4). They presented cell heterogeneity and response diversity to our chemo-gene treatments compatible with the clinical diversity of this disease [13–15]. However, a pattern emerging from our findings strongly suggests that, compared to a single treatment, the combination of gene transfer and BLM may have greater antitumor efficacy.

Thus, in the absence of a prognostic molecular analysis about the possible response of a given tumor to any therapy, the development of new combinations of treatment strategies could significantly target different cancer cell subpopulations overcoming treatment resistance.

In their dynamic and adaptive phenotype, melanoma cells switch from a highly proliferative, poorly invasive phenotype to a highly invasive, less proliferative and therapy resistant one [31,32]. As suggested by Melan A and gp100 melanoma antigen expression, and BRAF V600E mutation, the three cell lines exhibited a proliferative behavior [31,32,39]. Even hM4 cells, that displayed a wild type BRAF genotype, exhibited the highest basal PI. In agreement with this, the three human melanoma lines presented re-growth resistance to our chemo-gene treatments by enhancing the fraction of cells actively proliferating with high intracellular levels of ROS. A noteworthy finding was the correlation between the cytotoxicity of our chemo-genetic treatments and the fraction of cells exhibiting (i) high PI, and (ii) high intracellular levels of

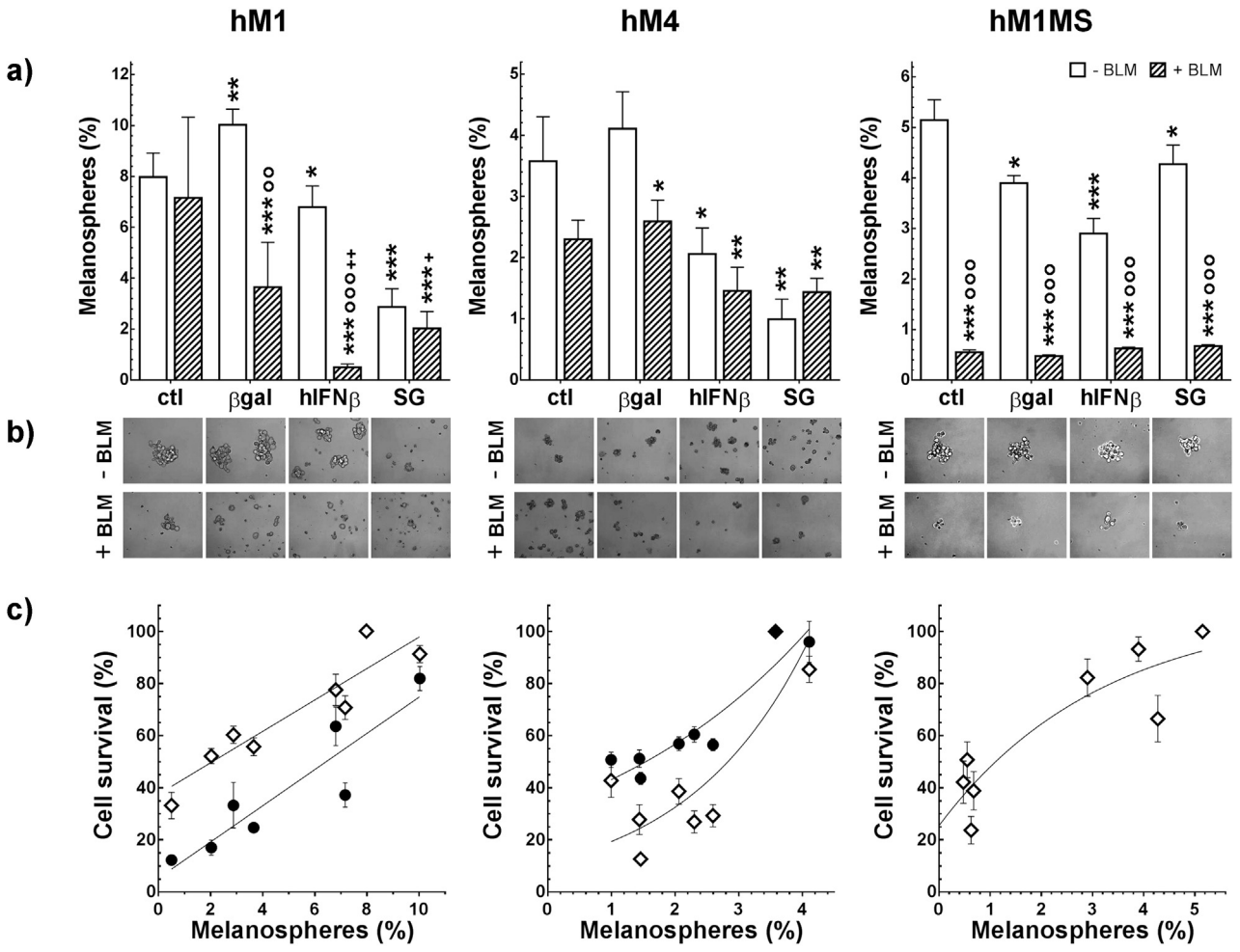

	hM1	mnl	sph	hM4	mnl	sph	hM1MS	mnl
c)	R^2	0.86 (lin) ***	0.835 (exp) **	R^2	0.632 (lin) *	0.859 (exp) **	R^2	0.759 (exp) **

Fig. 6. Melanosphere forming capacity of the surviving melanoma cells to SG (*HSVtk*/GCV) and *hIFNβ* lipofection in the absence or presence of BLM. Measurements were performed at day 6 (mnl) or 13 (sph) after seeding at low densities as described in Materials and methods. (a) The results represent the percentage of seeding cells as means ± s.e.m. of n = 6 (hM1), and n = 3 (hM1Ms and hM4) independent experiments. * *vs* their respective ctl; ° BLM *vs* their respective value without BLM; + BLM/genes combined treatments *vs* their respective ctl + BLM. (b) Representative examples of melanosphere forming capacity of treatments surviving cells as described in the bars plot. (c) Correlations between melanosphere forming capacity and cells survival (from Fig. 2) to all treatments in mnl (◇) or sph (●) determined by Pearson test with GraphPad Prism program.
One symbol: $p < 0.05$, two symbols: $p < 0.01$, three symbols: $p < 0.001$. See abbreviations in Fig. 2.

ROS. Along this line, there is evidence that melanomas that gave rise to the fastest growing tumors also had the lowest frequency (13%) of tumorigenic cells, whereas a melanoma that gave rise to slow growing tumors had a remarkably high frequency (70%) of tumorigenic cells [13]. Besides, it was reported that cells with high intracellular ROS levels are actively proliferating and more sensitive to therapy and differentiation [35]. Conversely, low ROS phenotype is a common property of cancer stem cells, required for the maintenance of their self-renewal capacity, quiescent state, high tumorigenicity and therapy resistance. Reversible cellular quiescence is a hallmark of stem cells. This ability protects these cells from a harsh environment and prevents their exhaustion imposed by constant cycling [40,41]. Also some reports demonstrate that higher ROS state is essential for proliferation of stem/progenitor cells [42,43]. Accordingly, it was suggested that increased intracellular ROS levels as a result of oxidative stress, inhibit self-renewal and induces differentiation of glioma tumor initiating cells (TIC) [11].

Our results suggest that, these chemo-gene treatments enhanced the fraction of more differentiated and treatment-sensitive cells. If this were the case, our treatments should decrease the sub-population of quiescent or slow cycling TIC. This was in fact observed in Figs. 5 and 6, where two functional keys of TIC, the clonogenic and the melanosphere forming capacity (MFC) of the survivor cells, almost disappeared after 6 days of BLM/genetic combined treatments.

Undoubtedly, an encouraging outcome was the high correlation between the fraction of cells surviving our chemo-genetic treatments with their (i) colony and (ii) melanosphere forming capacity in the three tested lines.

A very significant finding was that, the clonogenic capacity of the hM4 surviving cells disappeared after treatment with BLM alone or combined with genes. However, the same pool of hM4 cells surviving to BLM, formed melanospheres (MS) under non-adherent and serum-free conditions. Conversely, the epithelioid hM2 cells in complete medium: (i) readily formed multicellular

spheroids under non-adherent conditions and (ii) were able to proliferate from a clone in adherent conditions (Fig. 5), but (iii) were not able to form MS by clonal proliferation under serum-free non-adherent conditions. These data suggest that colony and melanosphere forming capacity could involve two different subpopulations of TIC. Consistently with this hypothesis it was reported that tumor stem cells maintained a spheroid-growing phenotype; while progenitor cells grew as an adherent phenotype in serum containing medium [35].

The hM1 cell line displayed higher melanosphere forming capacity than hM4 (Fig. 6c), suggesting a higher ratio of stem/progenitors among TIC [35]. This cell line formed bigger spheroids with multiple loosely associated cell aggregates like an association of numerous MS. However, combined BLM/genes treatments reduced their proportion to about 2% of the seeding cells, similar to that of hM4 cells.

In melanoma, the quiescent state appears to be necessary for retaining the self-renewal capacity of TIC. A significant reduction in the sphere-forming capacity of MS cells generated by combined treatments suggested that, BLM and the sustained expression of *IFNβ* and SG, reduced the melanoma TIC compartment by promoting long term TIC self-renewal, repopulating activity and differentiation. Thus, our chemo-gene treatments could affect the responding compartment and the cell status within each compartment controlling its plasticity.

All these data support the hypothesis that our chemo-gene treatments were able to eliminate TIC. Perhaps, by co-delivering lipid-complexed SG and *hIFNβ* gene together with BLM, we allowed an effective transfer of high doses of the drug to the tumor cells, overcoming TIC resistance. One of the factors contributing to TIC resistance to therapeutic agents is the presence of multiple drug resistance membrane transporters, such as the ATP-binding cassette (ABC) drug transporters. However, lipoplexes carrying our chemo-gene therapeutic agents enter the cell via endocytosis, an important mechanism that enables them to bypass ABC transporters [44,45,25].

It is worth to note that the *in vitro* lipofection of our chemo-gene therapeutic agents applied only once produced a significant cytotoxicity. Therefore, repeated *in vivo* intra tumor administrations of this treatment allowing a continuous and sustained local expression of SG and *hIFNβ* genes, in an immunestimulated microenvironment, could provide additional antitumor activity. The successful clinical outcome of our veterinary clinical trials in canine spontaneous melanoma patients is consistent with this premise. Direct intralesional injections of lipid-complexed plasmid DNA (lipoplex) encoding SG plus GCV yielded 62% and 46% of *in vivo* objective responses with 30% and 14% of complete responses [33]. This high proportion of tumor complete responses suggests that our SG therapy was able to eliminate TIC *in vivo*. In addition, our surgery adjuvant veterinary clinical trials combination of a systemic anti-cancer vaccine with local SG [33] and SG plus *cIFNβ* [21] delayed or prevented post-surgical recurrence and distant metastasis while significantly improved disease-free and overall survival of our canine patients.

All these data strongly suggest that our genetic treatment was able to, *in vitro* and *in vivo,* reduce TIC which ultimately drive tumor recurrence and metastatic disease, resulting in patient relapse [46].

Given that melanoma TIC recurrently change their surface marker proteins (that are characteristic in other tumors) keeping their TIC status [13], our results highlight the importance of tackling TIC with a wide-ranging functional treatment, instead of targeting individual genetic changes or certain profiles of cell surface marker proteins. Further studies to identify appropriate clinical and molecular markers of “stemness” are imperative to solve this puzzle.

Altogether, the results presented here suggest that the combined chemo-gene treatments could eradicate TIC, encouraging further *in vivo* studies for testing its possible translation to the clinic.

Disclosure of interest

The authors declare that they have no conflict of interest concerning this article.

Acknowledgments

We thank María D. Riveros and Graciela B. Zenobi for technical advice and assistance, Lina A. Marino for immunocytochemistry analysis, Martín A. Krasnapolski for mutations analysis and Liliana B Giménez for tumor biopsy samples. This study was partially supported by grants from ANPCYT/FONCYT (PICT2012-1738) and CONICET (PIP 112 201101 00627). MSV, MS, GCG and LMEF are investigators and CF fellow of the Consejo Nacional de Investigaciones Científicas y Técnicas (CONICET, Argentina).

References

[1] R. Siegel, K. Miller, A. Jemal, Cancer statistics, CA Cancer J. Clin. 65 (2015) 5–29.
[2] A.A. Tarhini, S.S. Agarwala, Cutaneous melanoma: available therapy for metastatic disease, Dermatol. Ther. 19 (2006) 19–25.
[3] L. Chin, L.A. Garraway, D.E. Fisher, Malignant melanoma: genetics and therapeutics in the genomic era, Genes Dev. 20 (2006) 2149–2182.
[4] K.T. Flaherty, BRAF inhibitors and melanoma, Cancer J. 17 (2011) 505–511.
[5] M.R. Girotti, F. Lopes, N. Preece, D. Niculescu-Duvaz, A. Zambon, L. Davies, S. Whittaker, G. Saturno, A. Viros, M. Pedersen, B.M. Suijkerbuijk, D. Menard, R. McLeary, L. Johnson, L. Fish, S. Ejiama, B. Sanchez-Laorden, J. Hohloch, N. Carragher, K. Macleod, G. Ashton, A.A. Marusiak, A. Fusi, J. Brognard, M. Frame, P. Lorigan, R. Marais, C. Springer, Paradox-breaking RAF inhibitors that also target SRC are effective in drug-resistant BRAF mutant melanoma, Cancer Cell 27 (2015) 85–96.
[6] F.S. Hodi, S.J. O'Day, D.F. McDermott, R.W. Weber, J.A. Sosman, J.B. Haanen, R. Gonzalez, C. Robert, D. Schadendorf, J.C. Hassel, W. Akerley, A.J. van den Eertwegh, J. Lutzky, P. Lorigan, J.M. Vaubel, G.P. Linette, D. Hogg, C.H. Ottensmeier, C. Lebbé, C. Peschel, I. Quirt, J.I. Clark, J.D. Wolchok, J.S. Weber, J. Tian, M.J. Yellin, G.M. Nichol, A. Hoos, W.J. Urba, Improved survival with ipilimumab in patients with metastatic melanoma, N. Engl. J. Med. 363 (2010) 711–723.
[7] R.H. Andtbacka, H.L. Kaufman, F. Collichio, T. Amatruda, N. Senzer, J. Chesney, K.A. Delman, L.E. Spitler, I. Puzanov, S.S. Agarwala, M. Milhem, L. Cranmer, B. Curti, K. Lewis, M. Ross, T. Guthrie, G.P. Linette, G.A. Daniels, K. Harrington, M.R. Middleton, W.H. Miller Jr., J.S. Zager, Y. Ye, B. Yao, A. Li, S. Doleman, A. VanderWalde, J. Gansert, R.S. Coffin, Talimogene laherparepvec improves durable response rate in patients with advanced melanoma, J. Clin. Oncol. 33 (2015) 2780–2788.
[8] L. Ossowski, J.A. Aguirre-Ghiso, Dormancy of metastatic melanoma, Pigm. Cell Melanoma Res. 23 (2010) 41–56.
[9] D. Paez, M.J. Labonte, P. Bohanes, W. Zhang, L. Benhanim, Y. Ning, T. Wakatsuki, F. Loupakis, H.J. Lenz, Cancer dormancy: a model of early dissemination and late cancer recurrence, Clin. Cancer Res. 18 (2011) 645–653.
[10] M.R. Alison, W.R. Lin, S.M.L. Lim, L.J. Nicholson, Cancer stem cells: in the line of fire, Cancer Treat. Rev. 38 (2012) 589–598.
[11] A. Sato, M. Okada, K. Shibuya, E. Watanabe, S. Seino, Y. Narita, S. Shibui, T. Kayama, C. Kitanaka, Pivotal role for ROS activation of p38 MAPK in the control of differentiation and tumor-initiating capacity of glioma-initiating cells, Stem Cell Res. 12 (2014) 119–131.
[12] E. Quintana, M. Shackleton, M.S. Sabel, D.R. Fullen, T.M. Johnson, S.J. Morrison, Efficient tumour formation by single human melanoma cells, Nature 456 (2008) 593–598.
[13] E. Quintana, M. Shackleton, H.R. Foster, D.R. Fullen, M.S. Sabel, T.M. Johnson, S.J. Morrison, Phenotypic heterogeneity among tumorigenic melanoma cells from patients that is reversible and not hierarchically organized, Cancer Cell 18 (2010) 510–523.
[14] M.J.C. Hendrix, E.A. Seftor, A.R. Hess, R.E.B. Seftor, Molecular plasticity of human melanoma cells, Oncogene 22 (2003) 3070–3075.
[15] R. Somasundaram, J. Villanueva, M. Herlyn, Intratumoral heterogeneity as a therapy resistance mechanism: role of melanoma subpopulations, Adv. Pharmacol. 65 (2012) 335–359.
[16] D. Klatzmann, Gene therapy for metastatic malignant melanoma: evaluation of tolerance to intratumoral injection of cells producing recombinant retroviruses carrying the herpes simplex virus type 1 thymidine kinase gene to be followed by ganciclovir administration, Hum. Gene Ther. 7 (1996) 255–267.
[17] S.M. Freeman, C.N. Abboud, K.A. Whartenby, C.H. Packman, D.S. Koeplin, F.L. Moolten, G.N. Abraham, The bystander effect: tumor regression when a

fraction of the tumor mass is genetically modified, Cancer Res. 53 (1993) 5274–5283.
[18] M.S. Villaverde, M.L. Gil-Cardeza, G.C. Glikin, L.M. Finocchiaro, Interferon-β lipofection II. Mechanisms involved in cell death and bystander effect induced by cationic lipid-mediated interferon-β gene transfer to human tumor cells, Cancer Gene Ther. 19 (2012) 420–430.
[19] U.A. Rossi, M.L. Gil-Cardeza, M.S. Villaverde, L.M. Finocchiaro, G.C. Glikin, Interferon-β gene transfer induces a strong cytotoxic bystander effect on melanoma cells, Biomed. Pharmacother. 72 (2015) 44–51.
[20] J. Atzpodien, K. Neuber, D. Kamanabrou, M. Fluck, E.B. Brocker, C. Neumann, T. M. Rünger, G. Schuler, P. von den Driesch, I. Müller, E. Paul, T. Patzelt, M. Reitz, Combination chemotherapy with or without s.c. IL-2 and IFN-alpha: results of a prospectively randomized trial of the Cooperative Advanced Malignant Melanoma Chemoimmunotherapy Group (ACIMM), Br. J. Cancer 86 (2002) 179–184.
[21] L.M.E. Finocchiaro, C. Fondello, M.L. Gil-Cardeza, U.A. Rossi, M.S. Villaverde, M. D. Riveros, G.C. Glikin, Cytokine-enhanced vaccine and interferon-β plus suicide gene therapy as surgery adjuvant treatments for spontaneous canine melanoma, Hum. Gene Ther. 26 (2015) 367–376.
[22] C. Jingyang, J. Stubbe, Bleomycins: towards better therapeutics, Nat. Rev. Can. 5 (2005) 102–112.
[23] K.G. Lau, Y. Hattori, S. Chopra, E.A. O'Toole, A. Storey, T. Nagai, Y. Maitani, Ultra-deformable liposomes containing bleomycin: in vitro stability and toxicity on human cutaneous keratinocyte cell lines, Int. J. Pharm. 300 (2005) 4–12.
[24] H. Mima, S. Yamamoto, M. Ito, R. Tomoshige, Y. Tabata, K. Tamai, Y. Kaneda, Targeted chemotherapy against intraperitoneally disseminated colon carcinoma using a cationized gelatin-conjugated HVJ envelope vector, Mol. Cancer Ther. 5 (2006) 1021–1028.
[25] M.L. Gil-Cardeza, U.A. Rossi, M.S. Villaverde, G.C. Glikin, L.M.E. Finocchiaro, Cationic lipid:DNA complexes allow bleomycin uptake in canine melanoma cells, Biomed. Pharmacother. 67 (2013) 269–275.
[26] A.K. Nowak, B.W. Robinson, R.A. Lake, Synergy between chemotherapy and immunotherapy in the treatment of established murine solid tumors, Cancer Res. 63 (2003) 4490–4496.
[27] R. Ramakrishnan, S. Antonia, D.I. Gabrilovich, Combined modality immunotherapy and chemotherapy: a new perspective, Cancer Immunol. Immunother. 57 (2008) 1523–1529.
[28] Z.G. Fridlender, J. Sun, S. Singhal, V. Kapoor, G. Cheng, E. Suzuki, S.M. Albelda, Chemotherapy delivered after viral immunogene therapy augments antitumor efficacy via multiple immune-mediated mechanisms, Mol. Ther. 18 (2010) 1947–1959.
[29] M.L. Gil-Cardeza, M.S. Villaverde, G.L. Fiszman, N.A. Altamirano, R.A. Cwirenbaum, G.C. Glikin, L.M.E. Finocchiaro, Suicide gene therapy on spontaneous canine melanoma: correlations between in vivo tumors and their derived multicell spheroids in vitro, Gene Ther. 17 (2010) 26–36.
[30] D. Raffo, D.E. Berardi, O. Pontiggia, L. Todaro, E.B. de Kier Joffé, M. Simian, Tamoxifen selects for breast cancer cells with mammosphere forming capacity and increased growth rate, Breast Cancer Res. Treat. 142 (2013) 537–548.
[31] K.S. Hoek, N.C. Schlegel, P. Brafford, A. Sucker, S. Ugurel, R. Kumar, B.L. Weber, K. L. Nathanson, D.J. Phillips, M. Herlyn, D. Schadendorf, R. Dummer, Metastatic potential of melanomas defined by specifi c gene expression profiles with no BRAF signature, Pigment Cell Res. 19 (2006) 290–302.
[32] S.K. Dissanayake, P.B. Olkhanud, M.P. O'Connell, A. Carter, A.D. French, T.C. Camilli, C.D. Emeche, K.J. Hewitt, D.T. Rosenthal, P.D. Leotlela, M.S. Wade, S.W. Yang, L. Brant, B.J. Nickoloff, J.L. Messina, A. Biragyn, K.S. Hoek, D.D. Taub, D.L. Longo, V.K. Sondak, S.M. Hewitt, A.T. Weeraratna, Wnt5A regulates expression of tumor-associated antigens in melanoma via changes in signal transducers and activators of transcription 3 phosphorylation, Cancer Res. 68 (2008) 10205–10214.
[33] L.M.E. Finocchiaro, G.C. Glikin, Cytokine-enhanced vaccine and suicide gene therapy as surgery adjuvant treatments for spontaneous canine melanoma: 9 years of follow-up, Cancer Gene Ther. 19 (2012) 852–861.
[34] S.C. Gupta, D. Hevia, S. Patchva, B. Park, W. Koh, B.B. Aggarwal, Upsides and downsides of reactive oxygen species for cancer: the roles of reactive oxygen species in tumorigenesis, prevention, and therapy, Antioxid. Redox Signal. 16 (2012) 1295–1322.
[35] C.W. Chang, Y.S. Chen, S.H. Chou, C.L. Han, Y.J. Chen, C.C. Yang, C.Y. Huang, J.F. Lo, Distinct subpopulations of head and neck cancer cells with different levels of intracellular reactive oxygen species exhibit diverse stemness, proliferation, and chemosensitivity, Cancer Res. 74 (2014) 6291–6305.
[36] M. Diehn, R.W. Cho, N.A. Lobo, T. Kalisky, M.J. Dorie, A.N. Kulp, D. Qian, J.S. Lam, L.E. Ailles, M. Wong, B. Joshua, M.J. Kaplan, I. Wapnir, F.M. Dirbas, G. Somlo, C. Garberoglio, B. Paz, J. Shen, S.K. Lau, S.R. Quake, J.M. Brown, I.L. Weissman, M.F. Clarke, Association of reactive oxygen species levels and radioresistance in cancer stem cells, Nature 458 (2009) 780–783.
[37] X. Shi, Y. Zhang, J. Zheng, J. Pan, Reactive oxygen species in cancer stem cells, Antioxid. Redox Signal. 16 (2012) 1215–1228.
[38] Y.Y. Mahller, J.P. Williams, W.H. Baird, B. Mitton, J. Grossheim, Y. Saeki, J.A. Cancelas, N. Ratner, T.P. Cripe, Neuro blastoma cell lines contain pluripotent tumor initiating cells that are susceptible to a targeted oncolytic virus, PLoS One 4 (2009) e4235.
[39] M.A. Davies, Y. Samuels, Analysis of the genome to personalize therapy for melanoma, Oncogene 29 (2010) 5545–5555.
[40] M. Tesio, A. Trumpp, Breaking the cell cycle of HSCs by p57 and friends, Cell Stem Cell 9 (2011) 187–192.
[41] T.H. Cheung, T.A. Rando, Molecular regulation of stem cell quiescence, Nat. Rev. Mol. Cell Biol. 14 (2013) 329–340.
[42] Y.Y. Jang, S.J. Sharkis, A low level of reactive oxygen species selects for primitive hematopoietic stem cells that may reside in the low-oxygenic niche, Blood 110 (2007) 3056–3063.
[43] M. Yoneyama, K. Kawada, Y. Gotoh, T. Shiba, K. Ogita, Endogenous reactive oxygen species are essential for proliferation of neural stem/progenitor cells, Neurochem. Int. 56 (2010) 740–746.
[44] J. Rejman, A. Bragonzi, M. Conese, Role of clathrin- and caveolea-mediated endocytosis in gene transfer mediated by lipo- and polyplexes, Mol. Ther. 12 (2005) 468–474.
[45] S. Resina, P. Prevot, A.R. Thierry, Physico-chemical characteristics of lipoplexes influence cell uptake mechanisms and transfection efficacy, PLoS One 4 (2009) e6058.
[46] T. Schatton, G.F. Murphy, N.Y. Frank, K. Yamaura, A.M. Waaga-Gasser, M. Gasser, Q. Zhan, S. Jordan, L.M. Duncan, C. Weishaupt, R.C. Fuhlbrigge, T.S. Kupper, M.H. Sayegh, M.H. Frank, Identification of cells initiating human melanomas, Nature 451 (2008) 345–349.